Pergamon

0301-9322(94)E0012-8

Int. J. Multiphase Flow Vol. 20, No. 4, pp. 789–798, 1994
Copyright © 1994 Elsevier Science Ltd
Printed in Great Britain. All rights reserved
0301-9322/94 $7.00 + 0.00

AN APPROXIMATE SOLUTION OF THE HYDRODYNAMIC PROBLEM ASSOCIATED WITH MOVING LIQUID–LIQUID CONTACT LINES

A. J. J. VAN DER ZANDEN† and A. K. CHESTERS

Laboratory of Fluid Dynamics and Heat Transfer, Eindhoven University of Technology, P.O. Box 513, Eindhoven, The Netherlands

(Received 15 February 1991; in revised form 2 February 1994)

Abstract—The same approach used by the authors in the context of advancing and receding contact lines is applied to the case of liquid–liquid contact lines. The result is an ordinary differential equation whose solution provides an approximate description of the shape of a moving meniscus. It is shown that a system with a viscosity ratio of 10^3 or more may be regarded as being a purely advancing/receding case. From the comparison of the present model with experimental results a dependence of the true contact angle on the line speed is inferred.

Key Words: wetting, dewetting, dynamic contact line

1. INTRODUCTION

While in the past advancing liquid–gas contact lines have been studied extensively, contact lines formed between two viscous liquids (liquid–liquid contact lines) have received attention only in recent years. For a review article on dynamic contact lines see for instance Dussan V. (1979) or de Gennes (1985).

When a viscous liquid advances over a smooth homogeneous solid displacing a gas of negligible viscosity, viscous forces have a strong influence on the meniscus shape, especially close to the wall. The meniscus profile has been studied using methods based on perturbation techniques (Hansen & Toong 1971; Huh & Mason 1977; Greenspan 1978; Kafka & Dussan V. 1979; Neogi & Miller 1982; Hocking & Rivers 1982; Cox 1986; de Gennes *et al.* 1990), or using a direct numerical (finite-element) solution (Lowndes 1980). If the classical concepts of viscosity and surface tension are maintained up to the contact line a singularity arises at the contact line. This singularity is often removed by supposing the liquid to slip in a small region near the contact line. Various slip models have been used, the mutual differences having only a minor influence on the total meniscus shape. An alternative approach to the hydrodynamic problem concerned has been developed by Boender *et al.* (1991) (henceforth referred to as paper I); this results in a second-order differential equation for the meniscus shape, based on a local-wedge approximation which is acceptable provided the meniscus inclination varies slowly with the distance from the wall. The singularity is avoided by taking account the fact that, at very small distances from the wall (of the order of molecular dimensions), the continuum concepts break down. At this distance the meniscus inclination reaches its final value, the true contact angle. In recent years the breakdown of continuum hydrodynamics has become a more and more popular solution to the singularity problem. Thompson & Robbins (1989) showed in a molecular dynamics study, that slip at the contact line appears to be associated with the breakdown of local hydrodynamics at molecular scales.

The approach to the hydrodynamic problem developed in paper I has been used by Chesters & van der Zanden (1992) (henceforth referred to as paper II) to describe receding contact lines, where a gas of negligible viscosity displaces a viscous liquid over a smooth homogeneous surface. A maximum "critical" capillary number at which a stable meniscus exists was established. A maximum speed of dewetting was also found in other investigations, both experimental and theoretical.

†Present address: Laboratory of Separation Technology, Eindhoven University of Technology, P.O. Box 513, Eindhoven, The Netherlands.

The hydrodynamic problem associated with a moving liquid–liquid contact line involves both an advancing and a receding fluid. It has been studied for a plane-interface geometry by Huh & Scriven (1971); once more a singularity arises at the actual contact line. A theoretical description for small line speeds, based on a perturbation approach and involving a matched asymptotic expansions technique, was given by Cox (1986). Measurements of the shape of a moving meniscus between two viscous liquids in a capillary tube have been performed by Fermigier & Jenffer (1988). The dynamic contact angle has been measured in very fine capillaries by Legait & Sourieau (1985) by measuring the pressure difference over a moving meniscus. A finite-element solution of the hydrodynamic problem for a number of line speeds and true contact angles has been given by Tilton (1988) and a finite-difference solution by Zhou & Sheng (1990), the singularity being avoided by introducing slip. Zhou and Sheng compared their predictions with the experimental results of Fermigier and Jenffer and concluded that, in some cases, the true contact angle at the wall depends on the contact line speed.

The aim of this article is to apply the approach used in papers I and II to describe advancing and receding contact lines to the case of liquid–liquid contact lines. In section 2, the local inclination of the meniscus is obtained as a function of the distance from the wall as the solution of a second-order, ordinary, differential equation. In section 3 the critical capillary number is determined for various systems. In section 4 the question is examined under which conditions the viscosity of the advancing or receding liquid may be neglected, so that the situation reduces to the purely receding or advancing case. Finally a comparison is made between the present model and, on the one hand, the finite-element solution of Tilton and the finite-difference solution of Zhou & Sheng (section 5) and, on the other, the experimental results of Fermigier & Jenffer (section 6). The latter comparison leads to an implied variation of the true contact angle as a function of line speed.

2. THE EQUATION GOVERNING A STEADILY MOVING MENISCUS BETWEEN TWO VISCOUS LIQUIDS

Plane geometry

The stream functions Ψ_R and Ψ_A of creeping liquid flows in two plane complementary wedges (one with wedge angle φ) with a constant velocity U prescribed on one boundary (Figure 1) have been given by Huh & Scriven (1971) in polar coordinates ρ and θ as

$$\Psi_R(\rho, \theta) = U\rho(a_R \sin\theta + b_R \cos\theta + c_R\theta \sin\theta + d_R\theta \cos\theta) \quad [1]$$

and

$$\Psi_A(\rho, \theta) = U\rho(a_A \sin\theta + b_A \cos\theta + c_A\theta \sin\theta + d_A\theta \cos\theta). \quad [2]$$

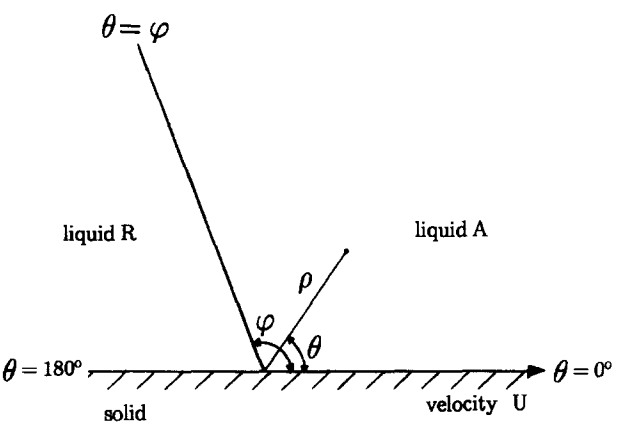

Figure 1. Viscous flow in plane complementary wedges adjoining a moving solid boundary.

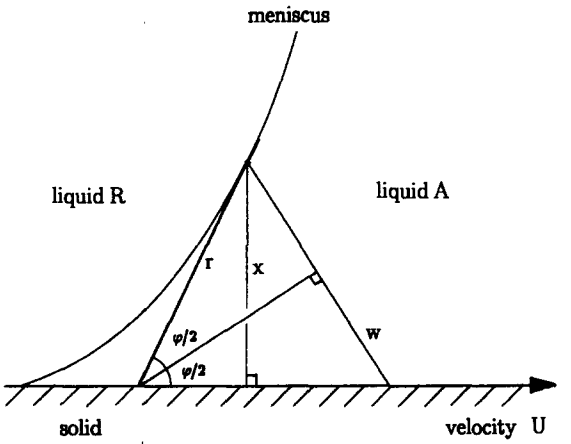

Figure 2. Definition of the variables describing a liquid–liquid meniscus.

For the coefficients $a_R \ldots d_A$ see the appendix (the subscripts R and A denoting receding and advancing). Using standard methods in fluid mechanics the pressures p in the liquids at the interface are found to vary (along the interface) as

$$\frac{\partial p_R}{\partial \rho} = U\frac{2\mu_R}{\rho^2}(c_R \sin\varphi + d_R \cos\varphi) \qquad [3]$$

and

$$\frac{\partial p_A}{\partial \rho} = U\frac{2\mu_A}{\rho^2}(c_A \sin\varphi + d_A \cos\varphi) \qquad [4]$$

where μ_R and μ_A are the respective liquid viscosities. The deviatoric component of the normal stress is zero. From [3] and [4], it follows that the pressure difference gradient at the interface is given by

$$\frac{\partial(p_R - p_A)}{\partial \rho} = U\frac{2\mu_R}{\rho^2}(c_R \sin\varphi + d_R \cos\varphi) - U\frac{2\mu_A}{\rho^2}(c_A \sin\varphi + d_A \cos\varphi). \qquad [5]$$

A moving meniscus between two parallel plates may be described by the coordinates r and φ (figure 2). In this case the wedge angle φ varies along the meniscus. Following the approach developed in papers I and II, the local pressure difference gradient $\partial(p_R - p_A)/\partial s$ (where s denotes arc length along the meniscus) will nevertheless be approximated by that at the interface between two plane wedges having the local inclination φ:

$$\frac{\partial(p_R - p_A)}{\partial s} = U\frac{2\mu_R}{r^2}(c_R \sin\varphi + d_R \cos\varphi) - U\frac{2\mu_A}{r^2}(c_A \sin\varphi + d_A \cos\varphi). \qquad [6]$$

Denoting the distance from the wall by x, [6] may be rewritten as

$$\frac{\partial(p_R - p_A)}{\partial x} = U\frac{2\sin\varphi}{x^2}(\mu_R c_R \sin\varphi + \mu_R d_R \cos\varphi - \mu_A c_A \sin\varphi - \mu_A d_A \cos\varphi). \qquad [7]$$

The pressure difference $p_R - p_A$ is balanced by the interfacial tension σ according to Laplace's law:

$$p_R - p_A = \frac{\sigma}{R} = \sigma\frac{d\varphi}{ds} = \sigma \sin\varphi \frac{d\varphi}{dx}, \qquad [8]$$

where R is the radius of curvature of the meniscus (reckoned positive if the centre of curvature lies on the side of liquid R). The derivative of [8] substituted in [7] now yields

$$\frac{d}{dx}\left(\sigma \sin\varphi \frac{d\varphi}{dx}\right) = U\frac{2\sin\varphi}{x^2}[\mu_R c_R \sin\varphi + \mu_R d_R \cos\varphi - \mu_A c_A \sin\varphi - \mu_A d_A \cos\varphi]. \qquad [9]$$

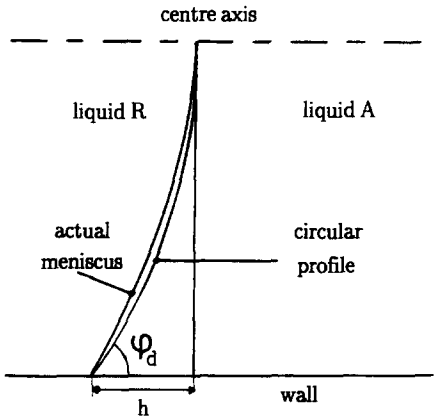

Figure 3. Definition of the dynamic contact angle, φ_d.

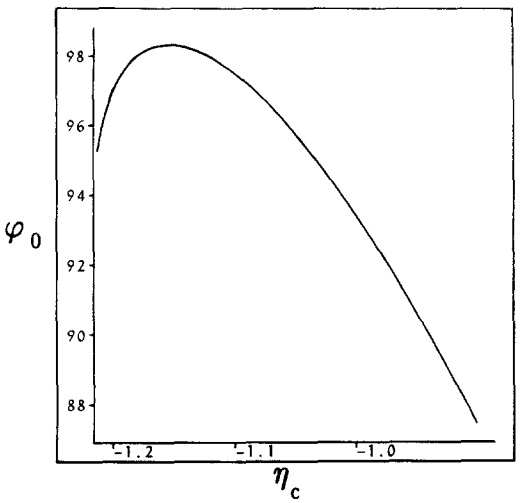

Figure 4. Variation of the true contact angle, φ_0, with the curvature at the axis, η_c ($\mu_R/\mu_A = 10^{-1}$, $Ca = 5 \times 10^{-2}$ and $\xi_c = 15$).

Written in terms of the capillary number, $Ca(= \mu_A U/\sigma)$ and the viscosity ratio μ_R/μ_A, [9] becomes

$$\frac{d}{dx}\left(\sin\varphi\frac{d\varphi}{dx}\right) = \frac{2\sin\varphi}{x^2}Ca\left[\frac{\mu_R}{\mu_A}c_R\sin\varphi + \frac{\mu_R}{\mu_A}d_R\cos\varphi - c_A\sin\varphi - d_A\cos\varphi\right]. \quad [10]$$

Equation [10] is the required differential equation describing the shape of the meniscus. Notice that the "constants" $c_R \ldots d_A$ depend on φ. The equation should constitute a good approximation provided φ varies "slowly", where slowly means something like:

$$\frac{d\varphi/\varphi}{ds/w} \ll 1 \quad [11]$$

(w = the local wedge width—figure 2).

Axisymmetric geometry

In the manner described in paper I, [10] can be modified to take account of the second radius of curvature present in the axi-symmetric (capillary-tube) case, yielding

$$\frac{d}{dx}\left(\sin\varphi\frac{d\varphi}{dx} + \frac{\cos\varphi}{a-x}\right) = \frac{2\sin\varphi}{x^2}Ca\left[\frac{\mu_R}{\mu_A}c_R\sin\varphi + \frac{\mu_R}{\mu_A}d_R\cos\varphi - c_A\sin\varphi - d_A\cos\varphi\right]. \quad [12]$$

where a denotes the tube radius.

Condition at the solid boundary

The meniscus equations [10] and [12] apply sufficiently far from the wall where the fluids behave "classically", being described by the continuum equations together with a constant interfacial tension. Close to the wall (minimally at a distance of the order of molecular dimensions) the continuum approximation inevitably breaks down due to the molecular character of the liquids. As in papers I and II, this will be modelled in the simplest possible manner, namely that the classical description applies up to a distance λ from the wall, of the order of a molecular dimension, at which point the final (true) value of the contact angle, φ_0, is attained. Note that the stress singularity otherwise encountered at $x = 0$ does not now arise.

3. SOLUTIONS OF THE GOVERNING EQUATION

In papers I and II only a small difference was found between the shapes of moving menisci in parallel plate and capillary-tube geometry, both in the advancing and in the receding case.

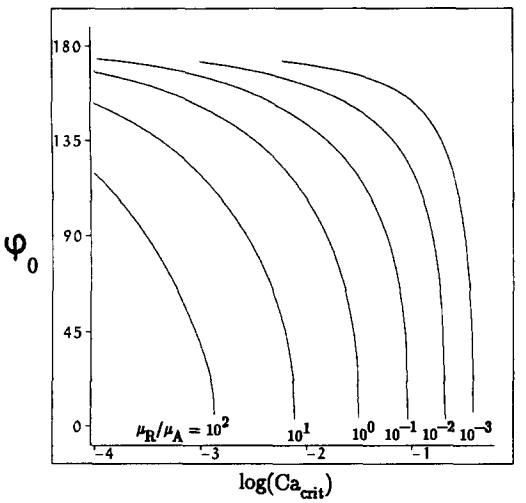

Figure 5. The dependence of the critical capillary number on the true contact angle, φ_0, for various viscosity ratios ($\xi_c = 15$).

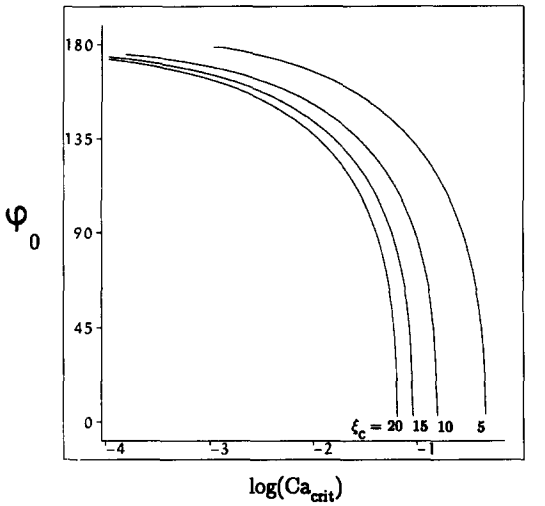

Figure 7. The dependence of the critical capillary number on the true contact angle, φ_0, for various system scales ($\mu_R/\mu_A = 10^{-1}$).

Consequently only the shape of a moving mensicus in a capillary will be examined in detail here. The analysis is however readily modified to the corresponding parallel-plate cases.

The meniscus equation [12] is solved as indicated in paper I, making use of a logarithmic scale of distance

$$\xi = \ln(x/\lambda), \qquad [13]$$

by numerically integrating from the centre axis ξ_c to the distance λ from the wall ($\xi = 0$) using a second-order finite-difference scheme. The subscript c will be used to identify a property on the axis of symmetry and the subscript 0 a property at $\xi = 0$. The integration procedure requires the values of φ_c and η_c where

$$\eta = \frac{d\varphi}{d\xi}. \qquad [14]$$

Symmetry requires that φ_c be 90°.

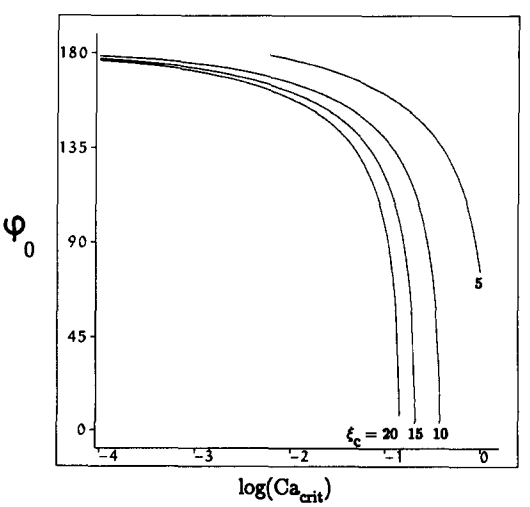

Figure 6. The dependence of the critical capillary number on the true contact angle, φ_0, for various system scales ($\mu_R/\mu_A = 10^{-2}$).

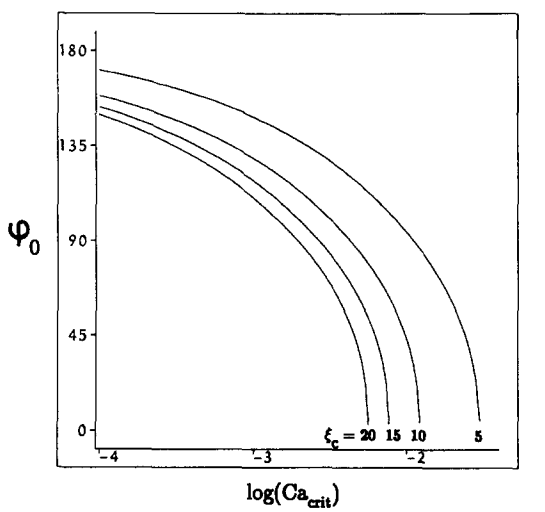

Figure 8. The dependence of the critical capillary number on the true contact angle, φ_0, for various system scales ($\mu_R/\mu_A = 10$).

The apparent or "dynamic" contact angle in the advancing fluid, φ_d, is taken as the angle which a circular meniscus, having the same apex height h as the actual meniscus, would make with the wall (figure 3):

$$\varphi_d = \cos^{-1}\left[\frac{2ha}{a^2+h^2}\right]. \qquad [15]$$

In figure 4 the true advancing contact angle (φ_0), obtained from the solution of [12], is presented as a function of $\eta_c(\mu_R/\mu_A = 10^{-1}, \mathrm{Ca} = 5 \times 10^{-2}$ and $\xi_c = 15$†). It is observed that φ_0 exhibits a maximum ($\varphi_{0,max}$). Evidently for $\varphi_0 > \varphi_{0,max}$ no solution to the meniscus equation [12] exists while for $\varphi_0 < \varphi_{0,max}$ there are two solutions. As in the receding case for the solutions having $d\varphi_0/d\eta_c > 0$ it was found that $d\eta_c/d(\mathrm{Ca}) > 0$ (for constant φ_0, ξ_c and μ_R/μ_A) and consequently that $d\varphi_d/d(\mathrm{Ca}) < 0$, which is contrary to experimental findings. The solutions for which $d\varphi_0/d\eta_c > 0$ will therefore be ignored. These solutions are presumably unstable and consequently not encountered in reality.

Another way of looking at this question is to note that for $\varphi_0 = \varphi_{0,max}$ the capillary number has a critical value ($\mathrm{Ca} = \mathrm{Ca}_{crit}$) above which no solution to the meniscus equation [12] exists, a film of the receding fluid being left behind on the tube wall.

In figure 5 the predicted relation between the critical capillary number and the true contact angle is presented for different values of $\mu_R/\mu_A(\xi_c = 15)$. If the receding phase becomes more viscous the critical capillary number becomes smaller. For a purely advancing case ($\mu_R/\mu_A = 0$) a solution of the meniscus equation exists for all capillary numbers and all values of the true contact angle. The viscosity of the receding liquid thus limits the range of the possible capillary numbers for which a stable meniscus exists. The ξ_c-dependence of the critical capillary number is presented in figures 6, 7 and 8 for the cases, $\mu_R/\mu_A = 10^{-2}$, $\mu_R/\mu_A = 10^{-1}$ and $\mu_R/\mu_A = 10$ with $\xi_c = 5$, 10, 15 and 20.

4. THE TRANSITION TO PURELY ADVANCING OR RECEDING BEHAVIOUR

Although a "purely" advancing/receding situation, corresponding to zero viscosity of the receding/advancing phase is formally unattainable a close approximation may be expected for sufficiently small/large values of the viscosity ratio μ_R/μ_A. To examine the transition to purely advancing behaviour, the predicted dynamic contact angle is presented in figure 9 as a function of the capillary number the viscosity ratios $\mu_R/\mu_A = 10^{-1}, 10^{-2}, 10^{-3}$ and $0(\varphi_0 = 45°, \xi_c = 15)$. It is seen that while the effect of a receding viscosity $\mu_R = 10^{-1}\,\mu_A$ may not be neglected, if $\mu_R = 10^{-2}\mu_A$ the moving contact line can be modelled as an advancing contact line except for the higher capillary numbers. For $\mu_R \leqslant 10^{-3}\mu_A$ the dynamic contact angle behaves as an advancing contact angle.

The transition to purely receding behaviour is examined in figure 10, as a function of the receding capillary number ($U < 0$ and consequently $\mathrm{Ca} < 0$) for the viscosity ratios $\mu_A/\mu_R = 10^{-1}, 10^{-2}, 10^{-3}$ and $0(\varphi_0 = 135°, \xi_c = 15)$. While the effect of the advancing viscosity $\mu_A = 10^{-1}\mu_R$ may not be neglected, deviations from purely receding behaviour are again small for $\mu_A = 10^{-2}\mu_R$ and negligible for $\mu_A \leqslant 10^{-3}\mu_R$.

5. COMPARISON WITH NUMERICAL SOLUTIONS

The shape of a moving meniscus between two equally viscous liquids ($\mu_A/\mu_R = 1$) in a capillary has been computed for a number of cases by Tilton (1988) using a finite-element method. In figure 11 the largest Ca cases treated by Tilton (crosses), for various true contact angles, are compared with the results obtained by integration of [12] from the tube axis to the wall (continuous lines)‡ (ξ_c was chosen as 15). The value of η_c has been chosen to optimize the agreement with the results obtained by Tilton.

†The order of magnitude corresponding to tubes of order 1 mm, assuming λ to be of the order of 1 nm.
‡Following Tilton, the shape of the moving meniscus is presented here as $1 - x/a$ vs $(h - h_{wall})/a$.

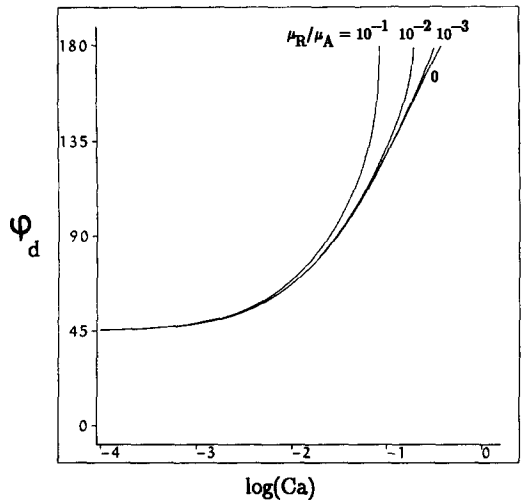

Figure 9. The dependence of the dynamic advancing contact angle on the viscosity of the receding fluid ($\xi_c = 15$, $\varphi_0 = 45°$).

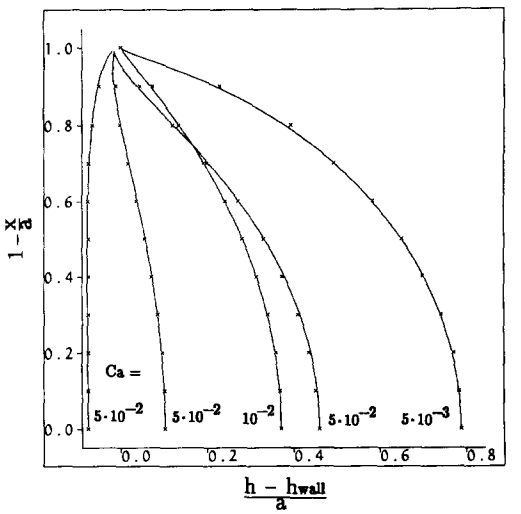

Figure 11. Comparison of the solution of the meniscus equation [12] (continuous lines) with the results obtained by Tilton (crosses) for the highest capillary numbers investigated and for various true contact angles.

As noted earlier, Tilton avoided the singularity at the contact line by introducing slip close to the contact line while in this study the singularity was avoided by invoking the breakdown of the continuum description. Close to the wall this difference in boundary condition may therefore result in a poor agreement between Tilton's results and the results obtained here.

In figure 11 it is observed that the agreement between the results obtained by Tilton and the solutions of meniscus equation [12] is excellent. This comparison however is not a critical test because there are only minor deviations form the spherical to be observed. Where these deviations occur, solutions of meniscus equation [12] are nevertheless in good agreement with Tilton's results. At the wall a small discrepancy is seen, which probably is the result of the different boundary conditions at the wall. For smaller capillary numbers the agreement may be expected to be better.

The Ca-dependence of the shape of a moving meniscus between two equally viscous liquids in a capillary has also been investigated by Zhou & Sheng (1990) using a finite-difference method. They too avoided the singularity at the contact line by using a slip model. Their values of $-h/a$

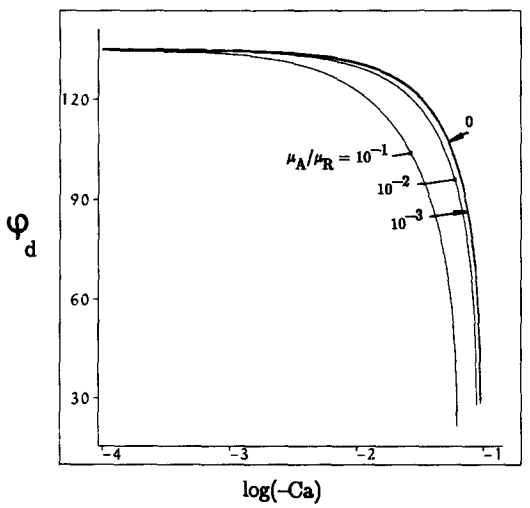

Figure 10. The dependence of the dynamic receding contact angle on the viscosity of the advancing fluid ($\xi_c = 15$, $\varphi_0 = 135°$). The line for $\mu_A/\mu_R = 10^{-3}$ almost coincides with the line for $\mu_A/\mu_R = 0$.

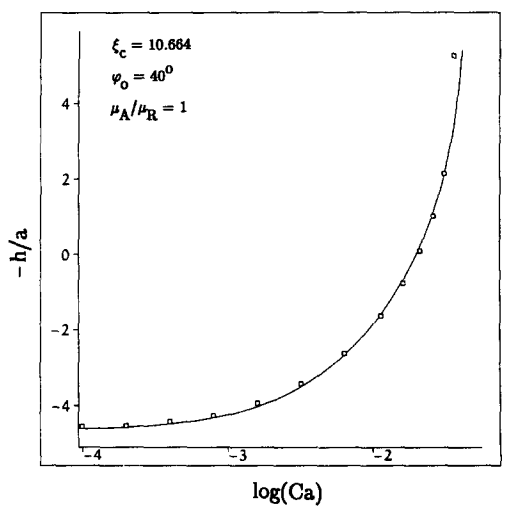

Figure 12. Comparison of the results of Zhou and Sheng (squares) with the predictions of the present model (continuous lines, $\xi_c = 10.664$, $\varphi_0 = 40°$, $\mu_A/\mu_R = 1$) giving the Ca-dependence of h/a (the meniscus height).

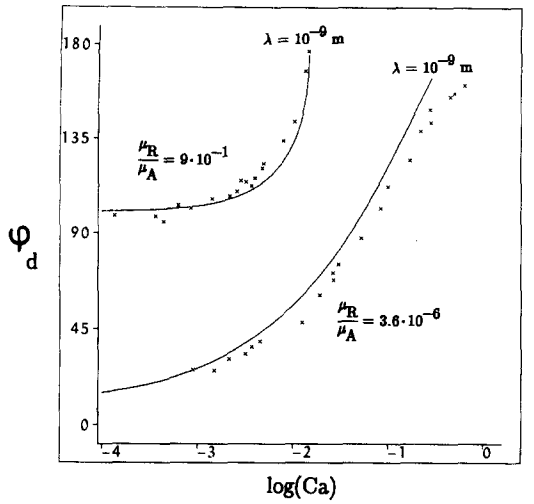

Figure 13. Capillary number dependence of the dynamic contact angle as measured by Fermigier and Jenffer (crosses) and as predicted by the meniscus equation [12] (continuous lines). Static contact angle = 100° and 12°.

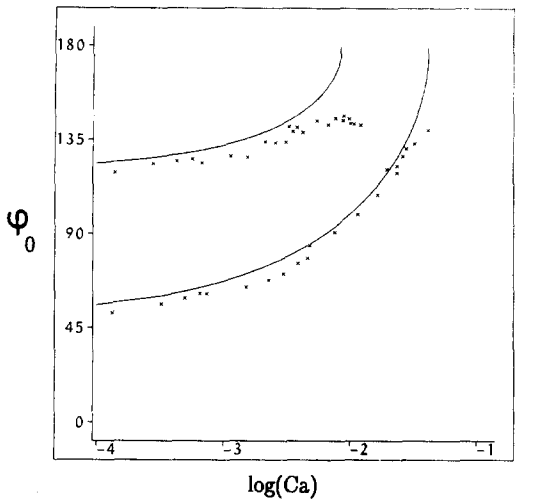

Figure 15. Variation of the true contact angle, φ_0, with Ca required to obtain agreement between computations and experiments: crosses, the present model ($\lambda = 10^{-9}$ m), continuous lines, computations of Zhou and Sheng.

as a function of Ca are compared in figure 12 with the predictions of the model ($\mu_A/\mu_R = 1$). It is clear that the model can predict the macroscopic meniscus shape, except possibly for very large Ca.

A comparison with experimental results, as carried out in the next section, may be more revealing and may provide insight into the nature of the boundary condition to be used at the wall.

6. COMPARISON WITH EXPERIMENTAL RESULTS

In figure 13 measurements performed by Fermigier & Jenffer (1988) of the dynamic contact angle of glycerol displacing a viscous silicon oil ($\mu_R/\mu_A = 9 \times 10^{-1}$) and of silicon oil displacing air ($\mu_R/\mu_A = 3.6 \times 10^{-6}$) in a capillary are compared with the predictions of the model presented here, based on the supposition that the true contact angle, φ_0, is constant and equals the static contact angle. λ was taken to be 10^{-9} m. The model exhibits agreement with these experimental results. In figure 14 further measurements of the dynamic contact angle of glycerol displacing low and

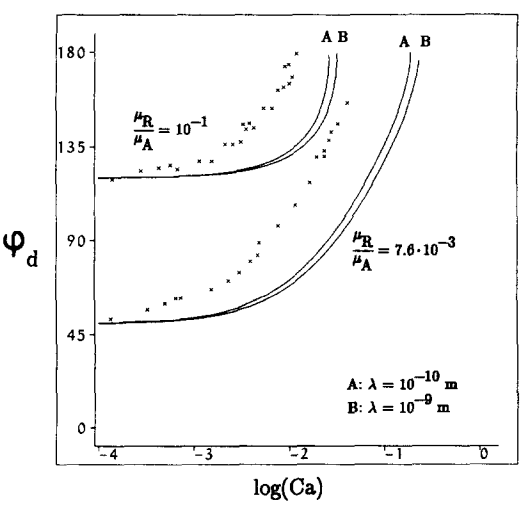

Figure 14. Capillary number dependence of the dynamic contact angle as measured by Fermigier and Jenffer (crosses) and as predicted by the meniscus equation [12] (continuous lines). Static contact angle = 120° and 50°.

moderate-viscosity silicon oils ($\mu_R/\mu_A = 7.6 \times 10^{-3}$ and $\mu_R/\mu_A = 10^{-1}$) are compared with the model ($\varphi_0 = \varphi_s$, $\lambda = 10^{-9}$ and 10^{-10} m). While agreement between experiment and model could be improved by chosing a much smaller value of λ the only physically realistic possibility is that in the cases in figure 14 the true angle at the wall depends significantly on the contact line speed, as was also concluded by Zhou & Sheng (1990). A line speed dependence of the true contact angle has also been suggested by Hoffman (1983). The true contact angle required to obtain agreement between model and experiments, taking $\lambda = 10^{-9}$ m, is shown in figure 15. A very similar conclusion, also shown in the figure, was reached by Zhou and Sheng. As might be anticipated, the implied true contact angle exhibits a strong dependence on the line speed. The mechanism of such line-speed dependence is however unknown and no explanation can at present be advanced for the fact that in the cases depicted in figure 13, such dependence is not in evidence.

7. CONCLUSION AND DISCUSSION

The approach developed earlier to resolve the hydrodynamic problem associated with liquid–gas contact lines is extended here to the liquid–liquid case. Since liquid–liquid contact lines always involve one receding liquid, they share the feature of receding liquid–gas contact lines that beyond a critical capillary number no stationary solution exists.

The agreement of the model with the computations of Zhou and Sheng is excellent and suggests that the models' representation of the hydrodynamics is good. Another test is formed by the experimental results of Fermigier and Jenffer. The good agreement obtained in some, but not all, cases if it is assumed that $\varphi_0 = \varphi_s$ confirms this impression but suggests that some other factor sometimes enters into the wall boundary conditions. While this additional factor may be a line-speed dependence of the true contact angle, there are other possibliities, such as effects of surface inhomogeneities or trace surfactants.

REFERENCES

BOENDER, W., CHESTERS, A. K. & VAN DER ZANDEN, A. J. J. 1991 An approximate analytical solution of the hydrodynamic problem associated with an advancing liquid–gas contact line. *Int. J. Multiphase Flow* **17,** 661–676.

CHESTERS, A. K. & VAN DER ZANDEN, A. J. J. 1992 An approximate solution of the hydrodynamic problem associated with receding liquid–gas contact lines. *Int. J. Multiphase Flow* **19,** 905–912.

COX, R. G. 1986 The dynamics of the spreading of liquids on a solid surface. Part 1. Viscous flow. *J. Fluid Mech.* **168,** 169–194.

DUSSAN V., E. 1979 On the spreading of liquids on solid surfaces: static and dynamic contact lines. *A. Rev. Fluid Mech.* **11,** 371–400.

FERMIGIER, M. & JENFFER, P. 1988 Dynamics of a liquid–liquid interface in a capillary. *Ann. Phys.* **13,** 37–42.

DE GENNES, P. G. 1985 Wetting: statics and dynamics. *Rev. Mod. Phys.* **57,** 827–863.

DE GENNES, P. G., HUA, X. & LEVINSON, P. 1990 Dynamics of wetting: local contact angles. *J. Fluid Mech.* **212,** 55–63.

GREENSPAN, H. P. 1978 On the motion of a small viscous droplet that wets a surface. *J. Fluid Mech.* **84,** 125–143.

HANSEN, R. J. & TOONG, T. Y. 1971 Dynamic contact angle and its relationship to forces of hydrodynamic origin. *J. Colloid Interface Sci.* **37,** 196–207.

HOCKING, L. M. & RIVERS, A. D. 1982 The spreading of a drop by capillary action. *J. Fluid Mech.* **121,** 425–442.

HOFFMAN, R. L. 1983 A study of the advancing interface II. Theoretical prediction of the dynamic contact angle in liquid–gas systems. *J. Colloid Interface Sci.* **94,** 470–486.

HUH, C. & MASON, S. G. 1977 The steady movement of a liquid meniscus in a capillary tube. *J. Fluid Mech.* **81,** 401–419.

HUH, C. & SCRIVEN, L. E. 1971 Hydrodynamic model of steady movement of a solid/liquid/fluid contact line. *J. Colloid Interface Sci.* **35,** 85–101.

KAFKA, F. Y. & DUSSAN V., E. B. 1979 On the interpretation of dynamic contact angles in capillaries. *J. Fluid Mech.* **95,** 539–565.

LEGAIT, B. & SOURIEAU, P. 1985 Effect of geometry on advancing contact angles in fine capillaries. *J. Colloid Interface Sci.* **107,** 14–20.

LOWNDES, J. 1980 The numerical simulation of the steady movement of a fluid meniscus in a capillary tube. *J. Fluid Mech.* **101,** 631–646.

NEOGI, P. & MILLER, C. A. 1982 Spreading kinetics of a drop on a smooth solid surface. *J. Colloid Interface Sci.* **86,** 525–538.

THOMPSON, P. A. & ROBBINS, M. O. 1989 Simulations of contact-line motion: slip and the dynamic contact angle. *Phys. Rev. Lett.* **63,** 766–769.

TILTON, J. N. 1988 The steady motion of an interface between two viscous liquids in a capillary tube. *Chem. Engng Sci.* **43,** 1371–1384.

ZHOU, M-Y. & SHENG, P. 1990 Dynamics of immiscible-fluid displacement in a capillary tube. *Phys. Rev. Lett.* **64,** 882–885.

APPENDIX

The coefficients $a_R \ldots d_A$ were found by Huh & Scriven (1971) to be:

$$a_R = -1 - \pi c_R - d_R$$

$$b_R = -\pi d_R$$

$$c_R = S^2[S^2 - \delta\varphi + R(\varphi^2 - S^2)]/D$$

$$d_R = SC[S^2 - \delta\varphi + R(\varphi^2 - S^2) - \pi \tan\varphi]/D$$

$$a_A = -1 - d_A$$

$$b_A = 0$$

$$c_A = S^2[S^2 - \delta^2 + R(\delta\varphi - S^2)]/D$$

$$d_A = SC[S^2 - \delta^2 + R(\varphi\,\delta - S^2) - R\pi \tan\varphi]/D$$

where $S \equiv \sin\varphi$, $C \equiv \cos\varphi$, $\delta \equiv \varphi - \pi$, $R \equiv \mu_R/\mu_A$ and

$$D \equiv (SC - \varphi)(\delta^2 - S^2) + R(\delta - SC)(\varphi^2 - S^2).$$

It deserves mention that Huh and Scriven use the stream function Ψ as in

$$v_\rho = -\frac{1}{\rho}\frac{\partial\Psi}{\partial\theta}, v_\theta = \frac{\partial\Psi}{\partial\rho},$$

where v_ρ and v_θ denote the velocities in the ρ and θ direction, respectively.